AIP | Applied Physics Letters

Observation of magnetism, low resistivity, and magnetoresistance in the near-surface region of Gd implanted ZnO

P. P. Murmu, J. Kennedy, G. V. M. Williams, B. J. Ruck, S. Granville et al.

Citation: Appl. Phys. Lett. **101**, 082408 (2012); doi: 10.1063/1.4747525
View online: http://dx.doi.org/10.1063/1.4747525
View Table of Contents: http://apl.aip.org/resource/1/APPLAB/v101/i8
Published by the American Institute of Physics.

Observation of magnetism, low resistivity, and magnetoresistance in the near-surface region of Gd implanted ZnO

P. P. Murmu,[1,2,3] J. Kennedy,[1,2,a)] G. V. M. Williams,[2,3] B. J. Ruck,[2,3] S. Granville,[2,4] and S. V. Chong[4]
[1]*National Isotope Centre, GNS Science, P.O. Box 31312, Lower Hutt 5010, New Zealand*
[2]*The MacDiarmid Institute for Advanced Materials and Nanotechnology, New Zealand*
[3]*School of Chemical and Physical Sciences, Victoria University of Wellington, P.O. Box 600, Wellington 6140, New Zealand*
[4]*Industrial Research Limited, P.O. Box 31310, Lower Hutt 5010, New Zealand*

(Received 25 June 2012; accepted 8 August 2012; published online 22 August 2012)

Ferromagnetic order is observed in Gd ion implanted ZnO crystals after annealing at 650 °C in a vacuum and we find that it is intrinsic and extends to depths of up to 40 nm. The ferromagnetic order is not affected by Gd for concentrations as high as 5% and possibly arises from defect clusters. Magnetoresistance is observed at low temperatures that may be due to spin-tunnelling between the defect clusters or spin-dependent scattering at the defect cluster interfaces. Gd implantation has an advantageous effect where it results in mΩ cm resistivities as well as significant electron doping. [http://dx.doi.org/10.1063/1.4747525]

Dilute magnetic semiconductors are promising materials with potential for spin transport electronic (spintronics) applications.[1] Several mechanisms have been proposed to explain the observation of ferromagnetic order and these include superexchange, double exchange, carrier-mediated Ruderman-Kittel-Kasuya-Yosida (RKKY) analyzed in terms of the Zener model,[2] and bound magnetic polarons.[3,4] There has been considerable interest in transition metal doped zinc oxide (ZnO), since Mn doping was theoretically predicted to display dilute magnetic semiconductor behaviour.[2] Ferromagnetic order was subsequently observed at room temperature and it has also been seen after doping with other transition metals including Co, Ni, Fe, Sc, Ti, Cr, V, and Cu.[3]

The observation of ferromagnetic order at and possibly above room temperature means that viable room temperature spintronics applications are feasible. However, there is considerable debate concerning the origin of the magnetic order especially since room temperature ferromagnetic order has also been observed in ZnO that does not contain any transition metal ions.[5,6] For example, room temperature ferromagnetism was reported in ZnO films made by pulsed laser deposition and grown at temperatures below 570 °C in a N_2 atmosphere.[5,6] It has been suggested that the intrinsic ferromagnetism arises from point defects (Zn or oxygen vacancies)[5–10] or from extended defects from the surface or grain boundaries that result in partial spin polarization.[8] Interestingly, room temperature ferromagnetism has been observed in ZnO crystals implanted with Gd ions at 620 K, and the ferromagnetism was attributed to indirect coupling between Gd ions.[11] Another study concluded that Gd doping into GaN leads to a very high magnetic moment ($\sim$4000 μ_B/Gd).[12] These intriguing observations require further study especially considering the debate concerning the origin of magnetic order in doped ZnO and whether it is intrinsic or extrinsic.

In this Letter, we report the results from a study on ZnO:Gd made by low-energy Gd ion implantation into ZnO crystals. Measurements were made on unimplanted ZnO before and after annealing in a vacuum at 650 °C as well as with different Gd implantation concentrations ranging from 0.7% to 12% before and after vacuum annealing at 650 °C. We show that the room temperature ferromagnetism occurs only after annealing and in a region extending $\sim$40 nm into the crystal where the ferromagnetism is intrinsic and possibly due to clusters of point defects. We discuss the effect of Gd doping on the magnetic order, resistivity, magnetoresistance (MR), and Hall effect data.

40 keV Gd ions were implanted into commercially available 0.5 mm thick hydrothermally grown ZnO (0001) crystals obtained from Semi-Wafer Inc. using the GNS Science low-energy ion implanter.[13] The Gd fluences ranged from 6.7×10^{14} to 3.0×10^{16} ions cm^{-2}, resulting in a 0.7 to 12 at. % Gd concentration in the near-surface region.[14] 18 keV Ar was also implanted at a fluence of 9×10^{15} ions cm^{-2} to enable a comparison between Gd and a chemically inert ion. The implanted samples were annealed in a high vacuum chamber ($\sim 10^{-7}$ mbar) at 650 °C for 30 min, along with an unimplanted ZnO crystal. Rutherford backscattering spectrometry measurements showed that the Gd concentration was peaked at 15 nm and extended to depths of up to $\sim$40 nm after annealing. Rutherford backscattering measurements made in the channeling mode on ZnO:Gd showed that for low Gd concentrations and as-implanted samples, the majority of the Gd atoms occupy Zn substitutional lattice sites. Annealing at 650 °C caused a significant rearrangement and a fraction of the Gd atoms were driven out of the substitutional sites.[14]

The magnetic properties were investigated using a superconducting quantum interference device (SQUID) magnetometer with magnetic fields applied parallel to the sample surface. Electronic transport measurements were made using a physical property measurement system (PPMS) and with the applied magnetic field parallel to the current. The

a)Author to whom correspondence should be addressed. Electronic mail: j.kennedy@gns.cri.nz.

resistivity, ρ, measurements were made using the four-contact method, and the Hall effect measurements were made using the van der Pauw method. The unimplanted ZnO single crystals before and after annealing had very large resistivities ($\sim$2 kΩ cm) and low carrier concentrations ($\sim 5 \times 10^{13}$ cm^{-3}). The corresponding resistances (>100 kΩ) were too large for variable temperature resistivity measurements to be made using the PPMS. The negligible change in resistivities and carrier concentrations before and after annealing show that there is no intrinsic doping induced in the unimplanted crystals by the annealing process.

Low magnetic field magnetization data are plotted in Fig. 1 for different Gd concentrations as a function of temperature where the moment was divided by the volume of the crystal. The unimplanted and unannealed ZnO crystal did not exhibit any ferromagnetic behaviour. However, annealing at 650 °C leads to hysteresis behaviour that is evidenced by a separation between the zero-field-cooled and field-cooled data for temperatures as high as 330 K. This is consistent with ferromagnetic order that was confirmed by magnetization measurements performed as a function of the applied magnetic field (not shown). The as-implanted ZnO:Gd crystals did not show ferromagnetic order, and ferromagnetism was only observed after annealing at 650 °C. The saturation magnetization at high magnetic fields (Fig. 1 inset) is nearly independent of the Gd concentration for concentrations as high as 5%, and it is nearly the same as that observed in the unimplanted and annealed crystal. Higher Gd concentrations lead to a reduction in the saturation magnetization and almost no ferromagnetism was observed for the 12% Gd crystal. Our magnetization measurements show that the ferromagnetism is intrinsic and may possibly be due to defects[5–10] or a rearrangement of the defects induced by annealing. This interpretation is also supported by magnetization measurements on the Ar implanted sample where ferromagnetic order was observed only after annealing. It can be seen in the inset to Fig. 1 that the saturation magnetization after Ar implantation and annealing is consistent with the trend observed after Gd implantation. It shows that implantation of magnetic (Gd) or nonmagnetic (Ar) ions have similar effects where high concentrations result in a reduction of the intrinsic magnetic order. The loss of ferromagnetism for high Gd concentrations implies that the intrinsic magnetic order occurs only from the near-surface region and within the Gd implantation depth (<40 nm). There is a reduction in the saturation magnetization at room temperature, which indicates that the Curie temperature is slightly higher than room temperature.

The zero-field-cooled magnetization data plotted in Fig. 1 shows a downturn below $\sim$50 K for the unimplanted ZnO crystal and for Gd concentrations as high as 12%. Furthermore, there is a systematic reduction in the magnetization for temperatures above $\sim$150 K. This behaviour is similar to that observed in superparamagnetic compounds.[15] It suggests that the ferromagnetism arises from small clusters of defects (possibly Zn or oxygen vacancies)[5–10] and leads to superparamagnetic behaviour. The broad plateau may be due to a distribution in cluster sizes that results in a distribution in blocking temperatures. The average blocking temperature appears to be $\sim$100 K. The 12% Gd implanted crystal shows a temperature dependent hysteresis that is significantly smaller than that observed for lower Gd concentrations while the saturation magnetization (Fig. 1 inset) is very small. This suggests that the 12% Gd crystal contains a small fraction of superparamagnetic defect clusters. The superparamagnetic interpretation of the data in Fig. 1 is further supported by magnetization measurements as a function of the applied magnetic field (not shown) where the 5 K data clearly show hysteresis for Gd concentrations less than 7.1% with a coercive field of $\sim$590 Oe and hysteresis is absent at 300 K.

Resistivity data from all of the Gd implanted and annealed ZnO single crystals are plotted in Fig. 2. The resistivity was obtained assuming current flow only within the Gd implantation depth of 40 nm. The resistivity is in the mΩ cm range and it is six orders of magnitude less than that observed in the unimplanted and annealed crystal ($\sim$2 kΩ cm). It is also three orders of magnitude less than that observed in the Ar implanted and annealed crystal (2.2 Ω cm). The low

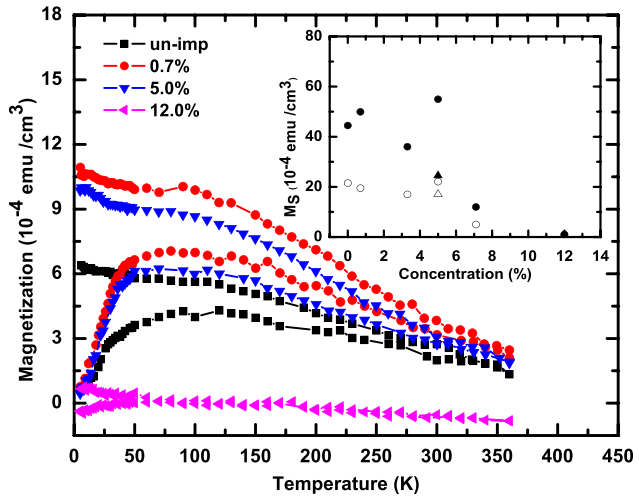

FIG. 1. Magnetization for unimplanted and Gd implanted ZnO single crystals at an applied field of 100 Oe after annealing at 650 °C. Inset: saturation magnetization at high magnetic fields for unimplanted and Gd implanted and annealed ZnO obtained from M(H) measurements at 5 K (filled circles) and 300 K (open circles). Also shown are similar data after Ar implantation at 5 K (filled triangles) and 300 K (open triangles).

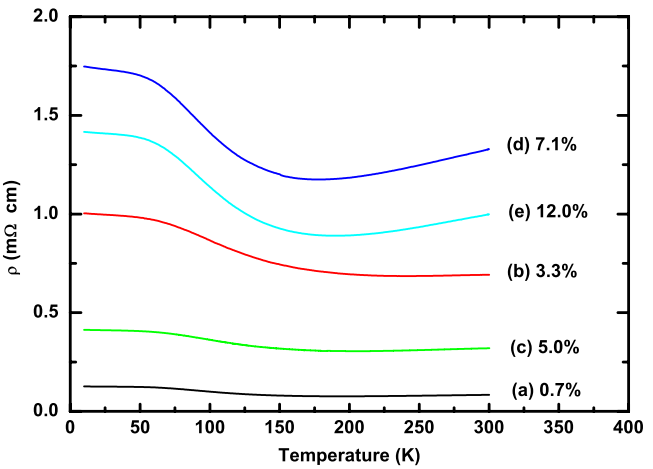

FIG. 2. Temperature dependent resistivity for Gd implanted and annealed ZnO.

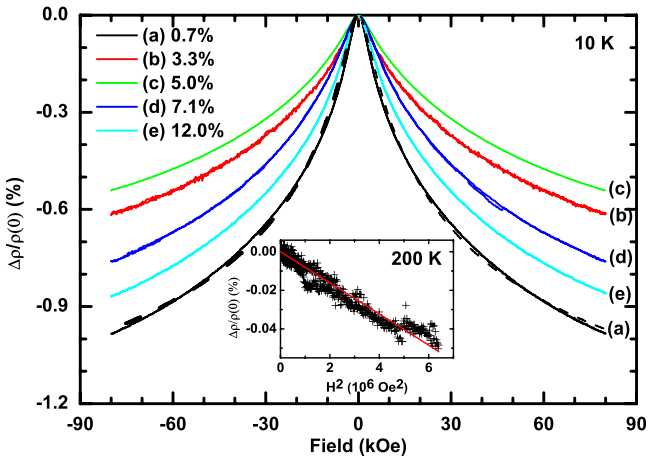

FIG. 3. Magnetoresistance at 10 K for Gd implanted and annealed ZnO (solid curves). Also shown is a fit to the 0.7% Gd implanted ZnO crystal assuming spin-tunnelling between ferromagnetic defect clusters (dashed curve). Inset: Plot of the magnetoresistance at 200 K against the square of the applied magnetic field (plus symbols). The line is a linear fit to the data.

resistivity is consistent with Gd implantation and annealing resulting in a heavily doped near-surface region. The magnitude of the resistivity does not show a clear trend with the implantation dose.

The MR at 10 K is plotted in Fig. 3 for all of the Gd implanted and annealed crystals where it can be seen that it is negative and reaches $\sim -1\%$ for the 0.7% Gd doped crystal. The magnetoresistance is plotted as $\Delta\rho(H)/\rho(0)$ where $\Delta\rho(H) = \rho(H) - \rho(0)$ is the change in resistivity, $\rho(0)$ is the initial resistivity, and H is the applied magnetic field. The magnetoresistance shows no clear dependence on Gd concentration, and hence it is unlikely to arise from any scattering or interaction with the Gd moments.

The magnetic field dependence of the magnetoresistance at 10 K is completely different from that observed at 200 K, which is in the superparamagnetic region. At 200 K, we find that $\Delta\rho/\rho(0) \propto -H^2$ as can be seen in the inset to Fig. 3 where the magnetoresistance is plotted against the square of the applied magnetic field. It is likely that the 200 K magnetoresistance arises from spin-flip scattering from isolated Gd or defect moments. This is because spin-flip scattering is expected to lead to $\Delta\rho/\rho(0) \propto -m(H)^2$, where $m(H)$ is the reduced magnetization.[16,17] At 200 K, the measured $m(H)$ strongly depends on the applied magnetic field and $m(H)$ saturates above $\sim$4 kOe and hence the magnetoresistance cannot be attributed to spin-flip scattering from superparamagnetic defect clusters. However, isolated Gd or defect moments have $m(H) \propto H$, and this leads to the observed $\Delta\rho/\rho(0) \propto -H^2$.

It is likely that the magnetoresistance at 10 K is due to spin-tunnelling between ferromagnetic defect clusters[18] or spin-dependent scattering at ferromagnetic defect cluster interfaces.[19] In the case of spin-dependent tunnelling, the magnetoresistance can be written as[18]

$$\frac{\Delta\rho}{\rho(0)} = -\frac{P^2 m(H)^2}{1 + P^2 m(H)^2}, \tag{1}$$

where P is the carrier spin polarized fraction. For low P, Eq. (1) reduces to $\Delta\rho/\rho(0) = -P^2 m(H)^2$ and has the same $\Delta\rho/\rho(0) \propto -m(H)^2$ that is expected for spin-dependent scattering at ferromagnetic cluster interfaces.[19] In well-ordered materials, $m(H)$ should be the measured reduced magnetization. The magnetization (not shown) saturates above $\sim$4 kOe; and hence for both cases, we would expect that the magnetoresistance should saturate above 4 kOe. However, this is not observed and we find that the magnetoresistance continues to decrease up to the maximum magnetic field of 80 kOe. This has also been observed in other granular compounds[20–23] and attributed to the magnetoresistance being dominated by spin-tunnelling in magnetically disordered regions between the grains[20–22] or magnetically disordered regions at and near the surface of nanoparticles.[23] It is possible that a similar mechanism occurs in our samples in which case $m(H)$ is the reduced magnetization at and near the surface of clusters rather than the measured $m(H)$. It is difficult to calculate the exact form of $m(H)$. However, in one study, it was shown that $m(H) = \exp(-a/H^{1/2})$ provides a reasonable fit to the magnetoresistance data.[22] This reduces to $m(H) \approx 1 - a/H^{1/2}$ at high fields, which has the reduced magnetization expected for a spin-glass with weak random anisotropy.[20,24] We show in Fig. 3 for the 0.7% Gd sample that if we use $m(H) = \exp(-a/H^{1/2})$, then we obtain a reasonable fit to the data (dashed curve) using Eq. (1) and with $P = 13.4\%$.

Hall-effect measurements were carried out on all Gd implanted and annealed crystals, and we find that electrons are the majority charge carriers. The carrier concentration at room temperature is $\sim 5 \times 10^{13}\,\mathrm{cm}^{-3}$ for the unimplanted crystal and this increases dramatically to $7.0 \times 10^{19}\,\mathrm{cm}^{-3}$ for 0.7% Gd, after which there is a small increase to $2.7 \times 10^{20}\,\mathrm{cm}^{-3}$ for 3.3% Gd, and then the carrier concentration saturates. This suggests that there is incorporation of Gd into the ZnO matrix that leads to electron doping for Gd concentrations less than $\sim$3.3%. However, this effect saturates for higher Gd concentrations.

The high carrier concentration in Gd doped ZnO is likely to be associated with an increase in the donor concentration from Gd implantation and/or intrinsic defects induced by Gd implantation such as zinc interstitials (Zn_I) and oxygen vacancies (V_O). The carrier concentration saturation at around 3.3% Gd ($3.9 \times 10^{15}\,\mathrm{Gd\,cm}^{-2}$) doping cannot be related to amorphization of ZnO. This is because Rutherford backscattering and channeling measurements on Gd doped ZnO have shown that the samples are well below the amorphization threshold for ZnO doped with up to $\sim 1.2 \times 10^{16}$ Gd cm^{-2}.[25] Kucheyev *et al.* also reported that ZnO has very high radiation resistance, and it remains partially crystalline for fluences as high 3.0×10^{16} Au cm^{-2}.[26]

Ar implantation also leads to an increase in the carrier concentration where Ar implantation with a fluence of 9.0×10^{15} ions cm^{-2} and 650 °C annealing resulted in a carrier concentration of $2.0 \times 10^{17}\,\mathrm{cm}^{-3}$. This is $\sim$4 orders of magnitude greater than that observed in the unimplanted crystal but it is $\sim$3 orders of magnitude less than that observed after Gd implantation. Ar implantation into ZnO is known to reduce the resistivity by 4 order of magnitude and increase the carrier concentration.[27] It has been suggested that Ar irradiation is likely to increase zinc interstitials, a major source of carriers, and they are stabilized in the

presence of oxygen vacancies. In our Ar doped ZnO samples, a similar effect may occur, which leads to a lower resistivity and higher carrier concentration than that observed in unimplanted and annealed ZnO crystals.

In conclusion, we observe room temperature ferromagnetism in ZnO single crystals implanted with Gd at low energies after annealing in a vacuum at 650 °C. By comparing unimplanted as well as annealed and unannealed crystals, we find that the ferromagnetism is intrinsic and occurs only after annealing and arises from a near-surface region that extends up to 40 nm into the crystals. The ferromagnetic order is not affected by Gd for Gd concentrations as high as 5%, but it is eventually destroyed for high Gd concentrations. The ferromagnetism is possibly due to point defects that have been predicted to lead to ferromagnetic order. The magnetization data can be interpreted in terms of superparamagnetism possibly due to small clusters of intrinsic defects. The resistivity and carrier concentrations do not show any correlation with the Gd concentration but we find that Gd implantation and annealing is advantageous for device applications because it leads to a large reduction in the resistivity as well as significant electron doping while still maintaining ferromagnetic order. The magnetoresistance at 10 K is found to be independent of the Gd concentration, and it is possibly due to spin-tunnelling between the intrinsic defect clusters or spin-dependent scattering from the surface of the defect clusters. Our results show that Gd implantation into ZnO followed by annealing is a possible method that can be used to create thin ferromagnetically ordered ZnO films with low resistivities and high n-type carrier concentrations.

We acknowledge funding from the Royal Society of New Zealand (VUW0917, 08-VUW-030), the Ministry of Science and Innovation (C05X0802, VICX0808), and the MacDiarmid Institute. Jibu Stephen is acknowledged for assisting during SQUID and PPMS measurements.

[1]S. A. Wolf, D. D. Awschalom, R. A. Buhrman, J. M. Daughton, S. von Molnr, M. L. Roukes, A. Y. Chtchelkanova, and D. M. Treger, Science **294**, 1488 (2001).
[2]T. Dietl, H. Ohno, F. Matsukura, J. Cibert, and D. Ferrand, Science **287**, 1019 (2000).
[3]F. Pan, C. Song, X. Liu, Y. Yang, and F. Zeng, Mater. Sci. Eng. R **62**, 1 (2008).
[4]C. Liu, F. Yun, and H. Morko, J. Mater. Sci.: Mater. Electron. **16**, 555 (2005).
[5]Q. Xu, H. Schmidt, S. Zhou, K. Potzger, M. Helm, H. Hochmuth, M. Lorenz, A. Setzer, P. Esquinazi, C. Meinecke *et al*., Appl. Phys. Lett. **92**, 082508 (2008).
[6]M. Khalid, M. Ziese, A. Setzer, P. Esquinazi, M. Lorenz, H. Hochmuth, M. Grundmann, D. Spemann, T. Butz, G. Brauer *et al*., Phys. Rev. B **80**, 035331 (2009).
[7]A. Sundaresan, R. Bhargavi, N. Rangarajan, U. Siddesh, and C. N. R. Rao, Phys. Rev. B **74**, 161306 (2006).
[8]A. L. Schoenhalz, J. T. Arantes, A. Fazzio, and G. M. Dalpian, Appl. Phys. Lett. **94**, 162503 (2009).
[9]G. Z. Xing, Y. H. Lu, Y. F. Tian, J. B. Yi, C. C. Lim, Y. F. Li, G. P. Li, D. D. Wang, B. Yao, J. Ding, Y. P. Feng, and T. Wu, AIP Adv. **1**, 022152 (2011).
[10]J. M. D. Coey, Solid State Sci. **7**, 660 (2005).
[11]K. Potzger, S. Zhou, F. Eichhorn, M. Helm, W. Skorupa, A. Mucklich, J. Fassbender, T. Herrmanns-Dorfer, and A. Bianchi, J. Appl. Phys. **99**, 063906 (2006).
[12]S. Dhar, O. Brandt, M. Ramsteiner, V. F. Sapega, and K. H. Ploog, Phys. Rev. Lett. **94**, 037205 (2005).
[13]J. Kennedy, D. A. Carder, A. Markwitz, and R. J. Reeves, J. Appl. Phys. **107**, 103518 (2010).
[14]P. P. Murmu, J. Kennedy, B. J. Ruck, A. Markwitz, G. V. M. Williams, and S. Rubanov, Nucl. Instrum. Methods Phys. Res. B **272**, 100 (2012).
[15]S. R. Shinde, S. B. Ogale, J. S. Higgins, H. Zheng, A. J. Millis, V. N. Kulkarni, R. Ramesh, R. L. Greene, and T. Venkatesan, Phys. Rev. Lett. **92**, 166601 (2004).
[16]K. Fischer, Phys. Status Solidi B **46**, 11 (1971).
[17]M. T. Beal Monod and R. A. Weiner, Phys. Rev. **170**, 552 (1968).
[18]J. Inoue and S. Maekawa, Phys. Rev. B **53**, R11927 (1996).
[19]S. Zhang and P. M. Levy, J. Appl. Phys. **73**, 5315 (1993).
[20]D. Serrate, J. M. De Teresa, P. A. Algarabel, M. R. Ibarra, and J. Galibert, Phys. Rev. B **71**, 104409 (2005).
[21]W. Wang, M. Yu, M. Batzill, J. He, U. Diebold, and J. Tang, Phys. Rev. B **73**, 134412 (2006).
[22]E. K. Hemery, G. V. M. Williams, and H. J. Trodahl, Physica B **390**, 175 (2007).
[23]D. Serrate, J. M. De Teresa, P. A. Algarabel, R. Fernández-Pacheco, J. Galibert, and M. R. Ibarra, J. Appl. Phys. **97**, 084317 (2005).
[24]J. Tejada, B. Martinez, A. Labarta, and E. M. Chudnovsky, Phys. Rev. B **44**, 7698 (1991).
[25]P. P. Murmu, R. J. Mendelsberg, J. Kennedy, D. A. Carder, B. J. Ruck, A. Markwitz, R. J. Reeves, P. Malar, and T. Osipowicz, J. Appl. Phys. **110**, 033534 (2011).
[26]S. O. Kucheyev, J. S. Williams, C. Jagadish, J. Zou, C. Evans, A. J. Nelson, and A. V. Hamza, Phys. Rev. B **67**, 094115 (2003).
[27]S. Chattopadhyay, S. Dutta, D. Jana, S. Chattopadhyay, A. Sarkar, P. Kumar, D. Kanjilal, D. K. Mishra, and S. K. Ray, J. Appl. Phys. **107**, 113516 (2010).